PERIODIC BEAM CURRENT OSCILLATIONS DRIVEN BY ELECTRON CYCLOTRON INSTABILITIES IN ECRIS PLASMAS*

O. Tarvainen†, T. Kalvas, H. Koivisto, J. Komppula, R. Kronholm, J. Laulainen,
University of Jyväskylä, Department of Physics, 40500 Jyväskylä, Finland
I. Izotov, D. Mansfeld, V. Skalyga,
Institute of Applied Physics - Russian Academy of Sciences (IAP-RAS), Nizhny-Novgorod, Russia
V. Toivanen, CERN, Geneva, Switzerland

Abstract

Experimental observation of cyclotron instabilities in electron cyclotron resonance ion source plasma operated in cw-mode is reported. The instabilities are associated with strong microwave emission and a burst of energetic electrons escaping the plasma, and explain the periodic oscillations of the extracted beam currents. The instabilities are shown to restrict the parameter space available for the optimization of high charge state ion currents.

INTRODUCTION

Plasma instabilities can be categorized to magnetohydrodynamic (MHD) instabilities driven by the topology of the magnetic field (see e.g. Ref. [1]) and kinetic instabilities triggered by the anisotropy of the electron energy distribution function (EEDF) (see e.g. Ref. [2]). The magnetic field topology of a minimum-B ECRIS is effective in suppressing MHD instabilities [3]. Due to the resonant interaction between the incident microwave radiation the EEDF of an ECRIS plasma is strongly anisotropic and is considered to consist of several 'electron populations' - cold, warm and hot electrons with average energies of 10 - 100 eV, 1 - 10 keV and 10 - 100 keV, respectively [4, 5]. Such non-equilibrium plasmas are prone to kinetic instabilities driven by the hot electrons whose transverse velocities $\vec{v} \perp \vec{B}$ dominate over the longitudinal velocities $\vec{v} \parallel \vec{B}$.

We have recently reported [6] an experimental observation of electron cyclotron instabilities in a minimum-B ECRIS plasma sustained by 14 GHz microwave radiation in cw-mode. The instabilities lead to ms-scale oscillation of the extracted beam current reported earlier in Refs. [7] and [8]. In this paper we present a review of earlier work [6] and provide new data explaining the nature of the instabilities.

THEORETICAL BACKGROUND

Electron cyclotron instabilities are driven by hot electrons interacting resonantly with electromagnetic plasma waves. Whistlers or slow extraordinary (Z-mode) waves propagating to (quasi)parallel direction with respect to the external magnetic field, i.e. $\vec{k} \parallel \vec{B}$, can be excited inside the ECR-zone where the plasma oscillation frequency ω_{pe} can exceed the electron gyrofrequency ω_{ce} [9]. The (quasi)perpendicular extraordinary X- or Z-modes with $\vec{k} \perp \vec{B}$ can be excited when $\omega_{pe} < \omega_{ce}$ [10].

A characteristic feature of electron cyclotron plasma instabilities is the emission of microwaves. The energy of the microwave emission E_μ can be described by mode-dependent growth and damping rates γ and δ as

$$\frac{dE_\mu}{dt} \approx \langle \gamma - \delta \rangle E_\mu. \quad (1)$$

The solution of the differential equation shows that the intensity of the microwave emission is an exponential function of the difference of the growth and damping rates, which depend on the mode of the microwave emission. Since the instabilities are triggered by the anisotropy of the EEDF, their (volumetric) growth rate is proportional to the ratio of hot and cold electron densities. The damping rate is determined by volumetric absorption of the wave energy by the collisional background plasma and external (wall) losses.

The balance equation [11] for the hot electron (number) density $N_{e,hot}$ can be written as

$$\frac{dN_{e,hot}}{dt} \approx -\kappa N_{e,hot} E_\mu + S(t) - L(t), \quad (2)$$

where κ is a coefficient [12] describing the amplification of the electromagnetic wave and corresponding decrease in the hot electron component due to direct energy loss, $S(t)$ is the source term of hot electrons, i.e. stochastic heating, and $L(t)$ is their loss term due to collisional velocity space diffusion, inelastic collisions and rf-induced pitch angle scattering [13, 14]. In quiescent steady-state ECRIS plasma the damping rate exceeds the growth rate and the source and loss terms of hot electrons cancel out. In unstable operation conditions $S(t) > L(t)$, which causes the anisotropy of the EEDF to increase until the condition $\gamma > \delta$ is met. At this threshold the hot electrons interacting with the resulting plasma wave emit microwave radiation and are expelled into the loss cone directly as a result of the interaction with the amplified plasma wave or shortly after the perturbation via stochastic cooling and/or collisional scattering. The increased flux of electrons from the trap results in a burst of wall bremsstrahlung. The process stabilizes the plasma due to reduced density of hot electrons. However, the instability

* Work supported by by the EU 7th framework program 'Integrating Activities - Transnational Access', project number: 262010 (ENSAR), Magnus Ehrnrooth foundation, the Academy of Finland under the Finnish Centre of Excellence Program 2012–2017 (Nuclear and Accelerator Based Physics Research at JYFL) and researcher mobility grants 267174 and 267227, and the Russian Foundation for Basic Research grants 12-02-31206 and 13-02-00951.

† olli.tarvainen@jyu.fi

ISBN 978-3-95450-158-8

appears again at a periodic interval corresponding to the characteristic time required to create necessary anisotropy of the EEDF and leads to oscillations of the extracted ion currents.

EXPERIMENTAL SETUP

The experimental data discussed in this article were taken with the A-ECR type JYFL 14 GHz ECRIS [15] operated in continuous (CW) mode. The following is a list of diagnostics tools that have been used for characterizing the instabilities and their effect on the extracted beam currents. Detailed description of each diagnostics method can be found from the given reference.

- Microwave detector diode (0.01 - 50 GHz, 10 ns resolution) connected to a WR75 waveguide port [6].
- 25 GHz oscilloscope (Tektronix, MSO72504DX), connected to a WR75 waveguide port.
- Bismuth germanate (BGO) scintillator coupled with a Na-doped CsI (300 - 600 nm) current-mode photomultiplier tube (PMT) with < 4 μs temporal resolution [6].
- Off-axis visible light collector coupled with Na-doped CsI PMT (300 - 600 nm) [6].
- Sectored Faraday cup ~5 m downstream in the beam line (< 5 μs resolution) [6, 8, 16].

These complementary signals yield information on the hot electrons interacting with the plasma EM-wave, bremsstrahlung (power) flux induced by electrons escaping the confinement, plasma dynamics and extracted, m/q-analyzed, beam currents.

RESULTS AND DISCUSSION

Ion beams extracted from ECR ion sources often suffer from periodic ripple at ms-scale. Figure 1 shows a representative example of O^{6+} beam current signal recorded with the JYFL 14 GHz ECRIS together with the corresponding Fourier spectrum. The source was operated with pure oxygen and 650 W of power at 14 GHz resulting to average O^{6+} current of 175 μA with a fluctuation of +8.6 /-12.4 μA i.e. total of 12% at 860 Hz.

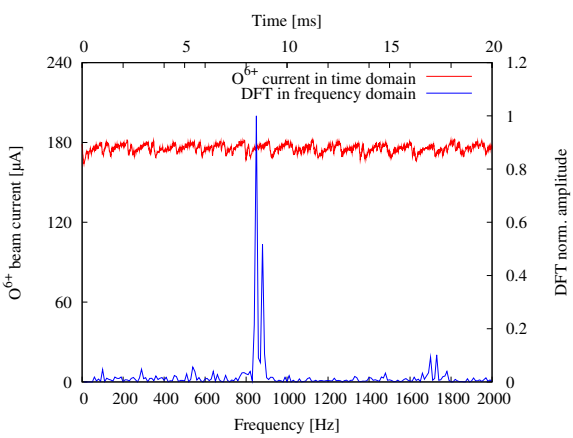

Figure 1: An example of O^{6+} beam current signal and corresponding Fourier transform (DFT) spectrum.

The 'sawtooth' behaviour shown in Fig. 1 consists of periodic drops followed by slower recovery phases of the beam current. An example of the diagnostics signals associated with the periodic plasma perturbations and drop of the beam current are presented in Fig. 2. The sequence of observable events is started at $t = 0$ by strong microwave emission from the plasma (a) lasting some hundreds of ns, coinciding with the leading edge of a bremsstrahlung burst (b) decaying in ~100 μs. The observed microwave signal associated with a burst of bremsstrahlung (electrons) is a signature of cyclotron instability, driven by hot electrons interacting resonantly with electromagnetic plasma waves, as described in the previous section.

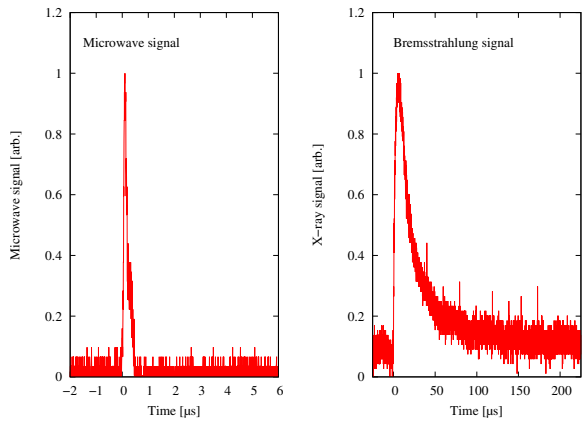

Figure 2: Microwave and X-ray (bremsstrahlung) signals associated with an onset of the periodic plasma instability.

The most critical tuning parameter affecting the occurrence of the cyclotron instabilities is the (solenoid) magnetic field strength. In the following we adopt the commonly used practice to quantify the strength of the ECRIS B-field by the ratio of the minimum field to the resonance field B_{min}/B_{ECR}. The effect of the magnetic field strength on the stability of the plasma is demonstrated in Fig. 3 showing the instability threshold value of B_{min}/B_{ECR} as a function of microwave power for different gaseous elements (He, Ar, Xe). The data for Fig. 3 were taken by adjusting the total extracted currents of different plasma species to be equal i.e. approximately 1.2 mA at 10 kV source potential suggesting that the plasma densities are approximately the same in each case. The error bars represent the step used for adjusting the magnetic field i.e. 5 A step in solenoid currents. The source potential (extraction high voltage) was not applied during the data taking. Increasing the magnetic field strength above the given threshold results in periodic onsets of the instabilities. This is most likely due to the fact that increasing the minimum-B lowers the gradient of the magnetic field at the resonance near the axis of the plasma chamber, which in turn results in increased energy gain in a single resonance crossing [17] and substantiates the anisotropy of the electron velocity distribution (EVD) triggering the instabilities. The shift of the instability threshold towards higher B_{min}/B_{ECR} (at given incident power level) with increasing mass number

ISBN 978-3-95450-158-8

could be due to increased electron energy loss in inelastic collisions.

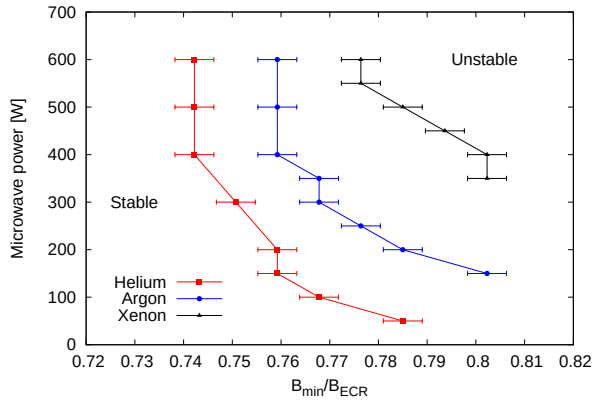

Figure 3: The instability threshold B_{min}/B_{ECR}-ratio of different plasmas as a function of incident microwave power.

The effect of neutral gas pressure on the threshold B_{min}/B_{ECR}-ratio, i.e. reduction of the instability threshold field with decreasing neutral gas pressure, is shown in Fig. 4. It was also observed that the high voltage applied for extracting the ions caused the threshold B-field to shift towards lower B_{min}/B_{ECR}-ratio. The effect of the high voltage is also demonstrated in Fig. 4 showing the threshold B_{min}/B_{ECR}-ratio for oxygen as a function of the applied source potential at three different neutral gas pressures and constant microwave power of 350 W. The error bars represent the step used for adjusting the magnetic field (5 A step). The given pressures are gas calibrated readings of an ionization gauge located outside the plasma chamber and connected to it through a radial diagnostics port.

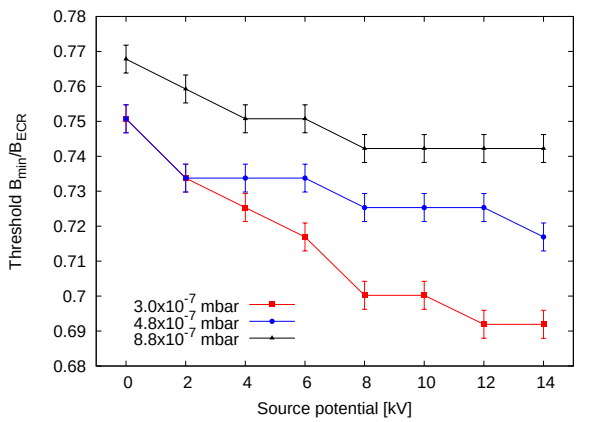

Figure 4: The instability threshold B_{min}/B_{ECR}-ratio of oxygen plasma as a function of the source potential.

The reduction of the threshold B_{min}/B_{ECR}-ratio with increasing source potential is believed to be due to the 'ion pumping effect', i.e. reduction of the neutral gas pressure and plasma density in the plasma chamber due to extracted ion beam, and subsequent decrease in the instability damping rate (reduced collision rate). This explanation is supported by the data in Fig. 5 showing the integrated visible light signal and total beam current extracted from the ion source as a function of applied high voltage. The recorded light emission of oxygen at 300 – 600 nm is dominated by emission lines of neutrals and ions up to the charge state O^{3+}. Thus, the visible light signal reflects the change in neutral gas balance (and density of low charge state ions). The presented example of the 'ion pumping' highlights the fact that the effect of source potential should always be taken into account in diagnostics of ECRIS plasmas.

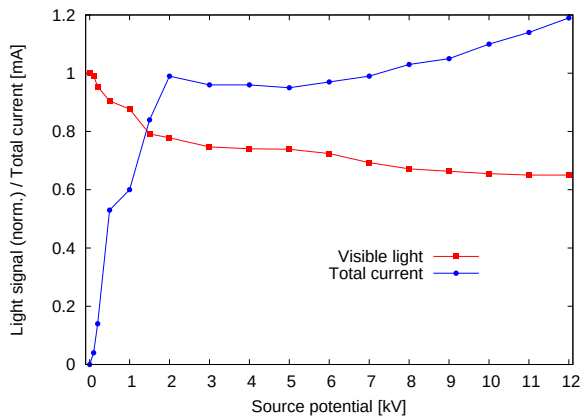

Figure 5: The visible light signal and total extracted current as a function of the source potential.

The repetition rate of the periodic instabilities at various B_{min}/B_{ECR}-ratios, incident microwave powers and neutral oxygen (O_2) pressures is presented in Fig. 6. The repetition rate increases substantially with increasing B_{min}/B_{ECR}-ratio and microwave power and decreases with increasing neutral gas pressure. The error bars represent the temporal fluctuation of the instability repetition rate at the given ion source setting. The tendencies shown in Fig. 6 can be explained qualitatively by interpreting the instability repetition rate as a measure of the stochastic electron heating rate as discussed in Ref. [6].

Finally, let us bring the discussion back to the beam current oscillations caused by the cyclotron instabilities. It is evident that the instability-induced burst of negative charge, expelled from the plasma, perturbs the density and charge state distribution of the extracted ion flux. The process differs fundamentally from the well-known afterglow burst of ECRIS plasmas [18] enhancing the high charge state ion flux to the extraction. The afterglow burst is caused by increased flux of cold electrons while the instabilities expel hot and warm electrons whose flux cannot be balanced only by a modest variation of the ambipolar potential. This claim is supported by the measurement [6] of the ion beam energy spread, $\Delta E/E$ of ~ 15% corresponding to a plasma potential $V_p > 1$ kV, during the instability-driven electron burst. The result was obtained by sweeping the m/q-analyzing magnet B-field and recording the corresponding current signals at μs-resolution with the Faraday cup. Thus, the observed drop of beam currents associated with the instabilities can

ISBN 978-3-95450-158-8

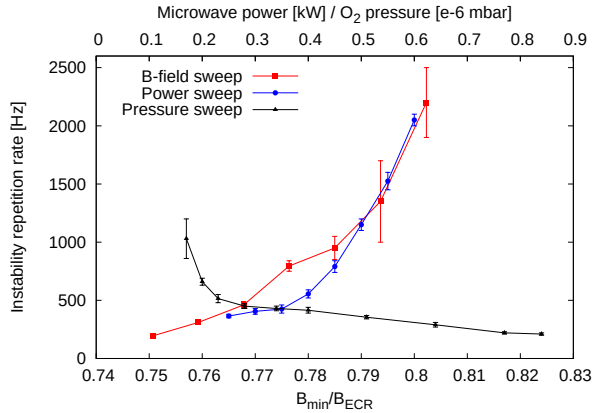

Figure 6: The repetition rate of the instabilities as a function of (i) B_{min}/B_{ECR}-ratio (350W, $3{\cdot}10^{-7}$ mbar), (ii) microwave power (B_{min}/B_{ECR} = 0.77, $3{\cdot}10^{-7}$ mbar) and (iii) oxygen pressure (B_{min}/B_{ECR} = 0.77, 350 W).

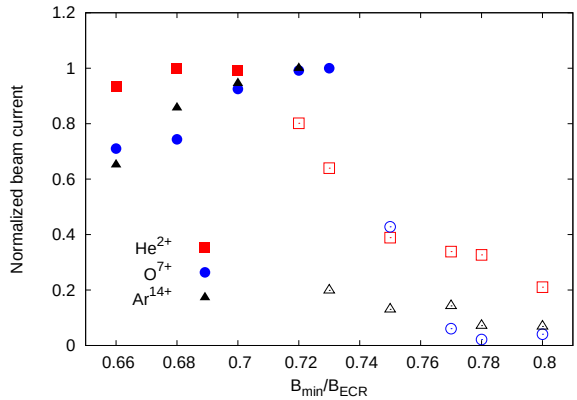

Figure 7: Normalized average beam currents of He^{2+}, O^{7+} and Ar^{14+} as a function of B_{min}/B_{ECR}-ratio. Solid symbols refer to stable operation and open symbols to existence of periodic cyclotron instabilities.

be explained at least partially by incorrect ion optics. A systematic quantification of the ion beam energy spread during the instability-driven electron burst at different ion source settings is one of the priorities of future experiments. This is due to the fact that such severe fluctuations of the plasma potential can cause degradation of the plasma chamber walls [19] by sputtering especially in afterglow operation mode in which instabilities are systematically observed [20] (independent of the source settings).

The cyclotron instabilities are detrimental to plasma confinement and extracted currents of highly charged ions as discussed in Ref. [6]. The ion source is typically tuned maximizing the temporally averaged beam current of a given charge state and, thus, the beam current oscillations at ~kHz frequencies are often obscured. For high charge state ion production improving the ion confinement time and enhancing the plasma density by increasing the magnetic field strength and/or microwave power are considered beneficial. However, such conditions make the plasma prone to instabilities that can limit the average extracted currents of highly charged ions and, hence, set restrictions for the parameter space available for their optimization. This is demonstrated in Fig. 7 showing an example of the normalized average currents of He^{2+}, O^{7+} and Ar^{14+} (high charge states) as a function of the B_{min}/B_{ECR}-ratio. The average beam current increases with the magnetic field strength until the instability threshold is reached and drops drastically as the magnetic field strength is increased further. Above this threshold the periodic disturbances of the plasma confinement occurring at temporal interval, which is shorter than the production time of the high charge state ions [21], limit the ion source performance. The presented example was obtained with 600 W microwave power and neutral gas pressures of $5.0{\cdot}10^{-7}$ mbar (He), $3.0{\cdot}10^{-7}$ mbar (O_2) and $3.4{\cdot}10^{-7}$ mbar (Ar).

Our future plans include a comprehensive study of the effects of cyclotron instabilities on the optimization of different charge states of various elements as well as analysis of the frequencies emitted during the plasma perturbations (data analysis in progress). Measurement of the instability frequency spectrum could help to identify the mode of the electromagnetic plasma waves.

REFERENCES

[1] J.B. Taylor, Phys. Fluids, 6, (1963), p. 1529.

[2] S.V. Golubev and A.G. Shalashov, Phys. Rev. Lett. 99, 205002, (2007).

[3] T. Antaya and S. Gammino, Rev. Sci. Instrum. 65, (1994), p. 1060.

[4] C. Barue, M. Lamoreux, P. Briand, A. Girard and G. Melin, J. Appl. Phys. 76, 5, (1994).

[5] G. Douysset, H. Khodja, A. Girard and J.P. Briand, Phys. Rev. E 61, 3, (2000).

[6] O. Tarvainen, I. Izotov, D. Mansfeld, V. Skalyga, S. Golubev, T. Kalvas, H. Koivisto, J. Komppula, R. Kronholm, J. Laulainen and V. Toivanen, Plasma Sources Sci. Technol. 23, 025020, (2014).

[7] O. Tarvainen, T. Kalvas, H. Koivisto, J. Komppula, V. Toivanen, C.M. Lyneis and M.M. Strohmeier, Proc. 20th Intl. Workshop on ECRIS (Sydney, Australia), TUXO02, http://accelconf.web.cern.ch/AccelConf/ECRIS2012/papers/tuxo02.pdf.

[8] V. Toivanen, O. Tarvainen, J. Komppula and H. Koivisto, J. Inst., JINST 8, T02005, (2013).

[9] A.G. Demekhov and V. Yu. Trakhtengerts, Radiophys. Quantum Electron. 29, (1986), p. 848.

[10] A. G. Demekhov, Radiophys. Quantum Electron. 30, (1987), p. 547.

[11] A.G. Shalashov, S.V. Golubev, E.D. Gospodchikov, D.A. Mansfeld and M.E. Viktorov, Plasma Phys. Control. Fusion 54, 085023, (2012).

[12] A.V. Vodopyanov, S.V. Golubev, A.G. Demekhov, V.G. Zorin, D.A. Mansfeld, S.V. Razin and A.G. Shalashov, J. Exp. Theor. Phys. 104, 2, (2007).

ISBN 978-3-95450-158-8

[13] C. Perret, A. Girard, H. Khodja and G. Melin, Phys. Plasmas 73, 3408, (1999).

[14] A. Girard, C. Pernot and G. Melin, Phys. Rev. E 62, 1, (2000).

[15] H. Koivisto, P. Heikkinen, V. Hänninen, A. Lassila, H. Leinonen, V. Nieminen, J. Pakarinen, K. Ranttila, J. Ärje and E. Liukkonen, Nucl. Instrum. Methods B 174, (2001), p. 379.

[16] O. Tarvainen, V. Toivanen, J. Komppula, T. Kalvas and H. Koivisto, Rev. Sci. Instrum. 85, 02A909, (2014).

[17] M.C. Williamson, A.J. Lichtenberg and M.A. Lieberman, J. Appl. Phys. 72, 1, (1992).

[18] F. Bourg, R. Geller and B. Jacquot, Nucl. Instrum. Methods A, 254, 13, (1987).

[19] D. Küchler, G. Bellodi, A. Lombardi, M. O'Neil, R. Scrivens, J. Stafford-Haworth and R. Thomae Proc. 20th Intl. Workshop on ECRIS (Sydney, Australia), TUPP10, http://accelconf.web.cern.ch/AccelConf/ECRIS2012/papers/tupp10.pdf

[20] I. Izotov, D. Mansfeld, V. Skalyga, V. Zorin, T. Grahn, T. Kalvas, H. Koivisto, J. Komppula, P. Peura, O. Tarvainen and V. Toivanen, Phys. Plasmas 19, 122501 (2012).

[21] R.C. Vondrasek, R.H. Scott, R.C. Pardo and D. Edgell, Rev.

ISBN 978-3-95450-158-8